IEEE Access
Multidisciplinary | Rapid Review | Open Access Journal

Received 27 December 2022, accepted 17 January 2023, date of publication 20 January 2023, date of current version 25 January 2023.

Digital Object Identifier 10.1109/ACCESS.2023.3238683

RESEARCH ARTICLE

Dual-Band Uniaxial Dielectric Anisotropy Sensor Using Coupled-Line Resonators

SHABNAM AHMADI ANDEVARI[1], JOSE-LUIS OLVERA-CERVANTES[2], HECTOR-NOEL MORALES-LOVERA[2], AND CARLOS E. SAAVEDRA[1]

[1]Department of Electrical and Computer Engineering, Queen's University, Kingston, ON K7L 3N6, Canada
[2]Instituto Nacional de Astrofisica, Optica y Electronica (INAOE), Puebla 72840, Mexico

Corresponding author: Shabnam Ahmadi Andevari (19saa6@queensu.ca)

This work was supported in part by the Natural Sciences and Engineering Research Council of Canada (NSERC) Strategic Project under Grant # RGPIN-2022-05204.

ABSTRACT In this paper, a new dual-band sensor to measure uniaxial anisotropy at two frequency bands is proposed. This sensor is composed of two dual-mode resonators separated by a T-shaped structure implemented in microstrip technology. The configuration of vertical and horizontal electric field lines for the two resonance modes allows for the characterization of a uniaxial anisotropic sample placed on top of the sensor. The resonance frequencies of different modes are separated using active S-parameters measured at the input port. They are subsequently used in the space mapping process to extract the dielectric constants of the sample in two directions, parallel and normal to the surface of the sensor, by means of electromagnetic analyses. The sensor is used to extract the dielectric constants of anisotropic FR4, RO4003C, and RO3010 samples at 2.4 and 3.4 GHz. An isotropic PTFE sample is also characterized to verify the reliability of the proposed method. Two single-band sensors are also implemented to measure RO3010 sample and the extracted dielectric constants are compared to those resulted from the proposed dual-band sensor.

INDEX TERMS Active S-parameters, anisotropy, characterization, dielectric, dual-band, resonator, sensor, space mapping, uniaxial.

I. INTRODUCTION

One of the defining properties of dielectric materials is their electric response to an externally applied electric field. A measure for this property is the dielectric permittivity of the material, which changes with the frequency of the applied field [1]. Many dielectric materials, such as composite substrates, some ceramic substrates, and many modern engineered artificial materials (including reinforced substrates, 3D-printed and multilayer structures, textile fabrics, and some metamaterials) exhibit dielectric anisotropy.

Anisotropy indicates that the dielectric response of matter depends on the direction of the applied electric field, so an anisotropic material has different dielectric permittivity values depending on the direction. Most of the anisotropic dielectric substrates used in RF and microwave circuits are identified as uniaxial anisotropic media. These substrates are characterized by two dielectric constants; one of which is in the direction parallel to the substrate surface ($\varepsilon_{\parallel}$) and the other one is along the direction normal to the substrate surface ($\varepsilon_{\perp}$). However, there is usually only one (ε) data which is near-to-transversal value, i.e., normal to the substrate surface available. Therefore, anisotropy is usually neglected in electromagnetic designs. Developing a well-grounded design of RF and microwave systems relies on having a precise knowledge of the utilized dielectric materials' properties, including their anisotropy. Therefore, microwave sensors characterizing the uniaxial dielectric anisotropy have been extensively studied.

In general, there are two different methods to measure the permittivity of materials: nonresonant methods and resonant methods. Resonant methods only characterize dielectric samples at a single frequency or several discrete frequencies. Many microwave sensors based on microwave resonators have been studied and the most recent ones are reviewed in [2]. On the other hand, nonresonant methods are capable of measuring the anisotropy in a wide frequency range, but they are not as accurate and sensitive as resonance-based

The associate editor coordinating the review of this manuscript and approving it for publication was Ali Karami Horestani.

sensors [3]. Nonresonant methods, including transmission and reflection methods, use the impedance and the propagation constant of a transmission line to determine the dielectric constant components [4], [5], [6]. These sensors are mainly used to get a general knowledge of the sample characteristics and accurate properties at distinct frequencies are extracted using resonant methods [7].

Resonant methods for anisotropy characterization, which are the focus of this paper, have been implemented with different technologies that fall into waveguide [7], [8], [9], [10] or planar circuit [11], [12], [13], [14]. In [8], a dielectric cavity resonator enclosing an anisotropic sample under test (SUT) inside is used. TE_{011}, HEM_{111}, and HEM_{112} modes, which have electrical field lines in two perpendicular directions, are used to excite the SUT. The sample anisotropy is discovered by solving the characteristic equations for these modes. The method reported in [8] needs an estimation of the dielectric properties of the sample to determine the proper dimensions of the sensor which can lead to finding the dielectric constant components at the desired frequency. It also extracts the two perpendicular dielectric constants at two different frequencies, corresponding to the resonance frequencies of different modes that are excited.

The sensor proposed in [12] uses coupled resonators implemented by microstrip lines, and the sample is a dielectric slab placed on top of the sensor, so a single sensor can be used to characterize different samples. In [7], a metallic cavity resonator in TE_{112} mode is used to implement the sensor. The two TE_{112} degenerate modes have electric fields perpendicular to each other, so they can be used to characterize a uniaxial dielectric sample. However, this method requires two measurements per sample; at the measurement of each dielectric constant component, only the corresponding mode resonates, and the other mode is eliminated by means of fine metallic needles. In this work, the sample size is a limitation since the electric field lines have an adequate orientation in a region of limited space within the cavity. The sensor proposed in [12] and [7] were successfully implemented to characterize the anisotropy of samples at a single frequency.

On the other hand, in [11], [13], and [15], a dual-mode strip line resonator is used for anisotropy characterization at multiple frequencies. For this, each mode of the resonator has a different distribution of horizontal and vertical directed fields. Using an electromagnetic analysis of the dual-mode resonator, the resonant frequencies of the modes are space mapped to the horizontal and vertical dielectric constants through an iterative process. The sensor in [11], [13], and [15] is a long resonator that has characterized an FR4 sample in seven frequencies, corresponding to the first to seventh-order resonance of the resonator. That sensor uses a destructive characterization method, since it is necessary to implement the sensor on each sample which is going to be characterized. Besides, the characterization frequency could not be defined, because the sensor is manufactured on an unknown material. Nevertheless, it has characterized the anisotropy of samples at a single frequency.

It is important to mention that the methods proposed in [8], [11], [13], and [15] were successfully tested for multiple frequencies, however, they are not flexible in the sense that they could characterize anisotropic samples at multiple frequencies but only one frequency could be established in the design of the sensor and the other frequencies are the multiple order harmonics. Additionally, the method proposed in [9] and [10] can also characterize anisotropic samples at multiple frequencies; they use different resonance modes of a cavity, so there is no freedom in choosing the second or third frequencies in these methods as well. In this context, in [16], an approach, based on the combination of two non-identical resonators placed in the inner part of the branches of a power divider, was proposed. This approach is flexible in the sense that the first and second frequencies are independent and they are defined by two non-identical split-ring resonators. The sensor proposed in [16] was successfully tested for liquid samples which are isotropic materials; this setup has the advantage that the sensor is used to test multiple samples simultaneously, and it reduces errors due to surrounding environmental factors, such as ambient temperature [2] and errors due to the number of measurements.

In this work, a dual-band sensor is proposed for anisotropy characterization. The sensor is designed on an isotropic substrate and is composed of two pairs of coupled resonators. We have used the resonators described in [11], [12], and [14] because they are straight lines, symmetrical to have even and odd modes, easy to manufacture and simple when performing the electromagnetic simulation. The two pairs of resonators share an input port through a T-shaped structure to separate the two frequency bands with high isolation. Each pair of coupled resonators has even and odd modes with different field distributions that can be attributed to the dielectric properties of samples placed on top of them. The uniaxial dielectric sample is characterized by an iterative process, space-mapping the dielectric constants of SUT to the resulting even and odd mode resonance frequencies. The even and odd resonance frequencies are required to be separated since they are very close and strongly coupled to each other that they sometimes overlap and cannot be distinguished in a mixed-mode analysis. Thus, in this paper, a method is proposed to separate even and odd mode resonances, which is based on the combination of active S-parameter, common mode and differential excitation. A prototype was successfully tested to extract the dielectric constants of anisotropic FR4, RO4003C, and RO3010 samples at 2.4 and 3.4 GHz.

II. DUAL-BAND SENSOR DESIGN

In uniaxial anisotropy measurements, the dielectric samples should be excited with fields in two perpendicular directions. Coupled Microstrip line resonators shown in Fig. 1(a), which are the foundation of the sensor proposed in this work, encompass two even and odd propagation modes.

Fig. 1(b) and (c) illustrate the electric field distribution in a transverse cross-section of the resonator for the even and odd modes, respectively. The even mode has electric field lines, for the most part, aligned in the axis perpendicular to the sensor. On the other hand, the odd mode has electric fields predominantly in the direction parallel to the sensor. Thus, this structure is capable of measuring the dielectric constant in the direction parallel to the surface of the SUTs ($\varepsilon_{\parallel}$), and in the perpendicular direction ($\varepsilon_{\perp}$), for a sample placed on top of the sensor.

To measure a uniaxial anisotropic dielectric at two frequencies, the three-port sensor shown in Fig. 2, which consists of two coupled microstrip line resonators and a diplexer, is used. The two coupled-line resonators are first designed and then they are connected to the input port using the diplexer.

The coupled-line resonators are designed on isotropic RT/duroid 5880 substrate, with dielectric constant (ε_r) of 2.2 ± 0.02, loss tangent of 0.0009, copper cladding thickness t of 18 um, and a dielectric thickness h of 0.79 mm. The dimensions of the resonators, $l_{1,2}$, $S_{1,2}$, and $W_{1,2}$, are determined using the equations presented in [17] to have resonance at two different frequency bands, around 2.4 GHz, and 3.4 GHz. Light coupling structures ($cs_{1,2}$), which are short lengths of lines placed at a modest distance from the resonators, are also added to be able to measure the resonance frequencies.

The T-shaped structure is designed to separate the two distinct frequency bands. It is a T-shaped structure composed of three sections of microstrip lines. Each section has a different characteristic impedance and length, which are chosen such that each branch is matched to the corresponding resonator at the middle of its frequency band and acts as an open circuit at the frequency band of the other resonator. The resonators are required to be symmetrical to have even and odd modes. Thus, the exact same lines are added to the other side of each coupled resonator to maintain the symmetry of the structure.

This structure combines Sensor 1 and Sensor 2. The isolated Sensor 1 exhibits good input return loss at f_{o1} and f_{e1} and reflection coefficients around f_{o2} and f_{e2} are along the outer edge of the Smith chart. A transmission line was added to the input of Sensor 1 to move the reflection coefficient of Sensor 1 at $(f_{o2} + f_{e2})/2$ to a point where the impedance is infinite; thus, Sensor 1 does not disturb the resonances f_{o2} and f_{e2} of Sensor 2 when the sensors are combined. In a similar way, a transmission line was added to the input of Sensor 2 to move the reflection coefficient of Sensor 2 at $(f_{o1} + f_{e1})/2$ to a point where the impedance is infinite; thus, Sensor 2 does not disturb the resonances f_{o1} and f_{e1} of Sensor 1 when the sensors are combined. To gain high isolation, the dimensions of the diplexer, $lf_{1,2}$, and $wf_{1,2}$ are optimized to have at least 40 dB isolation between the two resonators. Fig. 3 illustrates the measured S-parameters, showing the isolation between the resonators.

The resonance frequencies of each coupled resonator depend on their effective dielectric constant, which is a weighted average of the substrate dielectric constant and that of air, that covers the area on top of the sensor [11]. If we place a sample on top of the resonators, it changes the effective dielectric constant of the system. Therefore, a resonance frequency shift caused by the sample placement is observed. A significant point is that the samples should be placed in a location that has enough intensity of electric fields, so the field lines are in contact with the SUT and the sensitivity to the dielectric properties of the sample is ensured. The magnitude of the E-field on the coupled resonators at the center of each respective frequency band is shown in Fig. 4. The dimensions of SUTs, W_{S1}, L_{S1}, W_{S2} and L_{S2} shown in Fig. 2, should be chosen such that they cover the maximum field area. The samples are placed at the end of the coupled resonator lines, which are one of the regions of maximum electric field concentration [12].

To minimize the sample placement error, the determined sample position is marked out on the sensor layout. The markings, which are the small length of copper lines left on the sensor, have a negligible effect on the performance of the sensor, but notably, decrease the placement error. The fabricated sensor and the sensor loaded with samples are shown in Fig. 5. The S-parameters of the sensor with and without samples are measured using a vector network analyzer (VNA). To show that the placement error is removed, we have measured the sensor with FR4 samples four times and the results are thoroughly aligned, as illustrated in Fig. 6. The magnitude of the reflection coefficient at the input port (port 1 in Fig. 2) for the sensor loaded with different samples are compared to that of the unloaded sensor in Fig. 7. The unloaded sensor has four resonance frequencies at $f_{e1} = 2.343$ GHz, $f_{o1} = 2.506$ GHz, $f_{e2} = 3.308$ GHz, and $f_{o2} = 3.544$ GHz, corresponding to the even and odd modes of each coupled resonator. The resonance frequency shifts caused by the samples are visible in the S_{11} plots.

Although the sensor always has a dual-mode functionality, the resonance frequencies of the two modes are sometimes not distinguishable in the reflection coefficient, for example for the case with the FR4 samples in Fig. 7, which shows only two resonance frequencies. This is due to the fact that the even and odd resonance frequencies are very close and strongly coupled to each other, so they overlap [11]. In this case, it is necessary to separate the even and odd modes.

III. ANALYTIC MODELING

In this section, the approach to extract a conventional isotropic dielectric constant using the proposed dual-band sensor is discussed and then generalized for uniaxial dielectric anisotropy characterization. The method and all the equations are also expressed in a general form and are required to be applied to both dual-mode resonators constituting the sensor.

A. SEPARATING EVEN AND ODD RESONANCE FREQUENCIES

By using active S-parameters, we can replicate common and differential mode excitation and have the even and odd modes

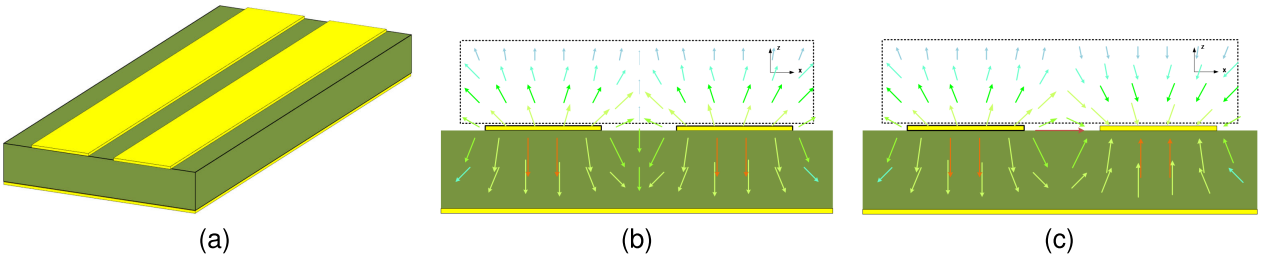

FIGURE 1. (a) Microstrip coupled line resonator. (b) The electric field distributions for the even mode. (c) The electric field distributions for the odd mode.

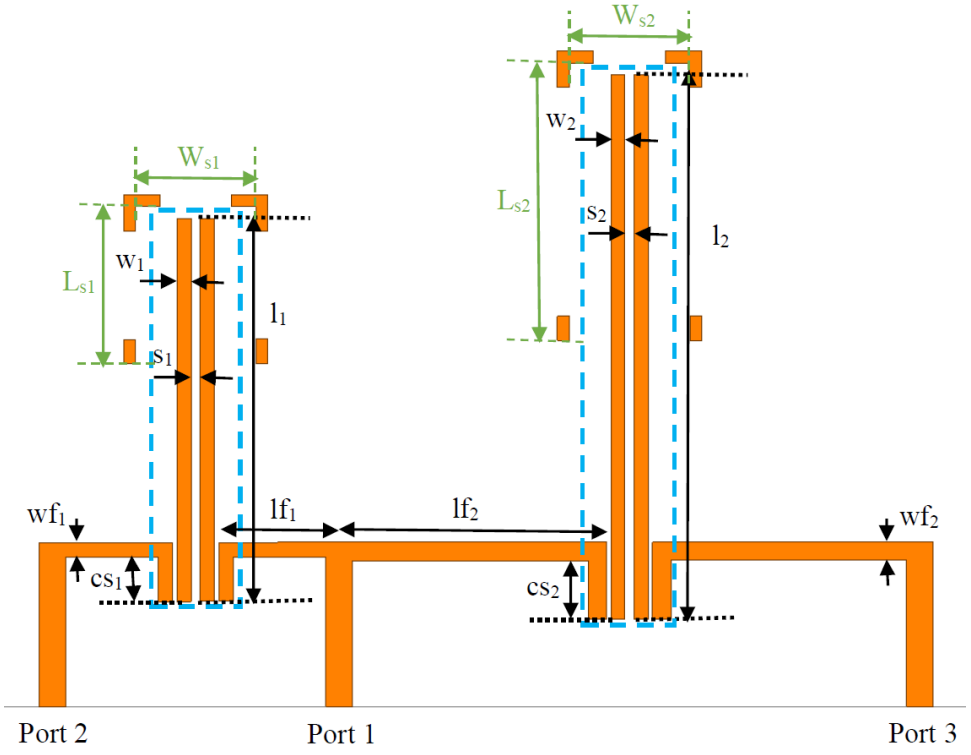

FIGURE 2. Dual-band uniaxial dielectric anisotropy sensor with dimensions: $l_1 = 31.74$ mm, $w_1 = 1.19$ mm, $s_1 = 0.75$ mm, $cs_1 = 3.71$ mm, $lf_1 = 10.10$ mm, $wf_1 = 1.19$ mm, $l_2 = 45.14$ mm, $w_2 = 1.14$ mm, $s_2 = 0.78$ mm, $cs_2 = 4.88$ mm, $lf_2 = 22.10$ mm, $wf_2 = 1.51$ mm, $L_{s1} = 13$ mm, $W_{s1} = 10$ mm, $L_{s2} = 23$ mm and $W_{s2} = 10$ mm.

separated. Active S-parameters are the reflection coefficient of one port when other ports are also excited. In a system containing N excitation ports, the active S-parameter in port m can be calculated using (1) [18], [19].

$$Active\ \boldsymbol{S}_{mm} = \frac{\sum_{n=1}^{N} \boldsymbol{S}_{mn}.A_n e^{j\phi_n}}{A_m e^{j\phi_m}} \tag{1}$$

In which, S_{mn} is the passive coupling coefficient between port m and n, and A_n and ϕ_n are the amplitude and phase of the nth excitation port, respectively. In this paper, to calculate the active S_{mm}, ϕ_m is always considered to be 0 and the other ϕ_ns are considered as a phase shift with reference to ϕ_m.

To separate the modes of the first resonator (the resonator at the left-hand side) shown in Fig. 2, ports 1 and 2 are considered to have A1=A2=1 and A3=0 and active S_{11} or S_{22} is used.

$$Active\ \boldsymbol{S}_{11} = \boldsymbol{S}_{11} + \boldsymbol{S}_{12}.e^{j\phi_2} \tag{2}$$

$$Active\ \boldsymbol{S}_{22} = \boldsymbol{S}_{22} + \boldsymbol{S}_{21}.e^{j\phi_1} \tag{3}$$

And for the mode separation of the second resonator (the resonator at the right-hand side), active S_{11} or S_{33} when A1=A3=1 and A2=0 is used.

$$Active\ \boldsymbol{S}_{11} = \boldsymbol{S}_{11} + \boldsymbol{S}_{13}.e^{j\phi_3} \tag{4}$$

$$Active\ \boldsymbol{S}_{33} = \boldsymbol{S}_{11} + \boldsymbol{S}_{31}.e^{j\phi_1} \tag{5}$$

Note that the diplexer is designed such that each coupled resonator acts as an open circuit at the frequency band of the other resonator, so each resonator is a symmetrical system, having an even and odd mode. To obtain the even mode resonance, the two active ports are treated as having the same

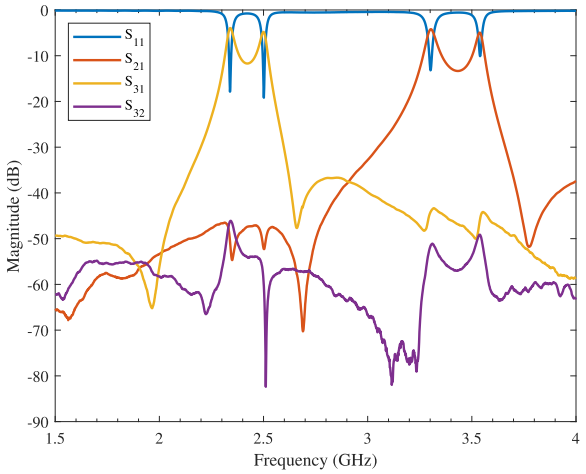

FIGURE 3. Measured frequency response of the sensor.

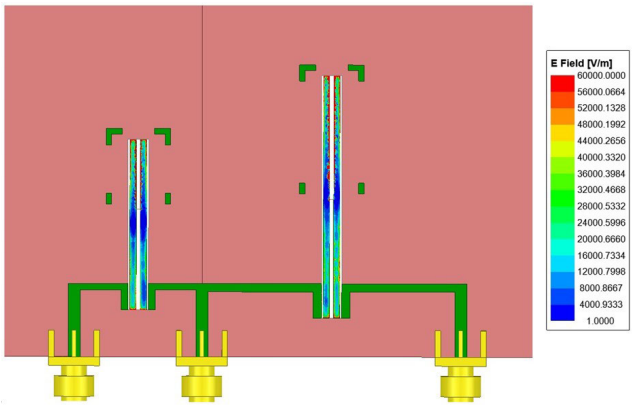

FIGURE 4. The simulated magnitude of E-field at the center frequencies of coupled resonators (at 2.4 GHz for the left-hand-side resonator and at 3.4 GHz for the right-hand-side resonator).

phase (ϕ_ns in (2), (3), (4), and (5) equal to 0) in addition to the same magnitude, thus appearing as if a common mode excitation is applied to the two ports of the symmetrical resonators. Thus, the odd mode is suppressed and only the even mode resonance frequency appears. On the other hand, the odd mode is attained by considering a 180° phase shift between the two active ports having the same magnitude (ϕ_ns in (2), (3), (4), and (5) equal to 180). This can be thought of as applying a differential mode excitation to the symmetrical resonators, which leads to removing the even mode resonance frequency, and acquiring the separated odd resonance frequency.

The transformation from the passive mixed-mode S-parameters to the active even and odd separated modes is implemented with MATLAB. The mixed mode and separated modes of the unloaded sensor are shown in Fig. 8 and 9. The measured S-parameters are used to plot these figures. Fig. 8 shows the data for the case where ports 1 and 2 are active. As expected, the first part of the active S_{11} in Fig. 8(a) remains unperturbed in this case, because the even mode excitation is only applied to the first resonator and the second one is isolated. But, the resonance frequencies of the first sensor, which are around 3.4 GHz, are separated. At each mode, only one resonance is observed, which is the resonance frequency corresponding to that mode. The active S_{22} shown in Fig. 8(b) can also be used. Since ports 2 and 3 are isolated from each other, the resonance frequencies of the first resonator are only visible in this curve. Similar to active S_{11}, each plot represents only one resonance frequency, which shows the even and odd mode is successfully separated. Fig. 9 presents the same data, but for the second resonator, when ports 1 and 3 are active.

B. ISOTROPIC MODELING AND GENERALIZATION TO UNIAXIAL ANISOTROPY

As mentioned before, there is a correspondence between the resonance frequencies of the resonators and the effective dielectric constant of the sensor. Assuming first an isotropic sample, the dielectric constant of the SUT can be established as the qualitative equation in (6), in which ε_{SUT} is the dielectric constant of the isotropic sample, A is a proportionality constant, and f_r is the resonance frequency of the sensor [11].

$$\varepsilon_{SUT} = \frac{A}{f_r^2} \tag{6}$$

For uniaxial anisotropic samples, the dielectric constants in 6 are replaced by a weighted sum of the parallel and perpendicular dielectric constant components [11]. As illustrated before in Fig. 1, parallel and perpendicular electric fields have different ratios in each mode, resulting in the even mode being more dependent on $\varepsilon_\perp$ and the odd mode more dependent on $\varepsilon_\parallel$. Thus, the even and odd resonance frequencies can be written as Eq. 7 and 8, in which A_{ij}s are proportionality constants, f_e and f_o are the resonance frequency of the sensor (first or second resonator) in even mode and odd mode, respectively [11], [12].

$$A_{\parallel e}\varepsilon_\parallel + A_{\perp e}\varepsilon_\perp = f_e^{-2} \tag{7}$$

$$A_{\parallel o}\varepsilon_\parallel + A_{\perp e}\varepsilon_\perp = f_o^{-2} \tag{8}$$

If we evaluate two cases with two different anisotropic samples, first with dielectric constants $\varepsilon_{\parallel a}$ and $\varepsilon_{\perp a}$ and second with dielectric constants $\varepsilon_{\parallel b}$ and $\varepsilon_{\perp b}$, the resulting even and odd resonance frequencies can be used to discover the proportionality constants as follows:

$$\begin{bmatrix} A_{\parallel e} & A_{\perp e} \\ A_{\parallel o} & A_{\perp o} \end{bmatrix}^{-1} = \begin{bmatrix} \varepsilon_{\parallel a} & \varepsilon_{\parallel b} \\ \varepsilon_{\perp a} & \varepsilon_{\perp b} \end{bmatrix} \begin{bmatrix} f_{ea}^{-2} & f_{eb}^{-2} \\ f_{oa}^{-2} & f_{ob}^{-2} \end{bmatrix}^{-1} \tag{9}$$

Given the measured resonant frequencies of the sensor (f_{em} and f_{om} of the first resonator or second resonator) and the calculated A matrixes in (9), (7) and (8) are solved for the dielectric constants $\varepsilon_{\parallel m}$ and $\varepsilon_{\perp m}$ (at the first or second frequency band) that correspond to the measured resonant frequency. Therefore, the dielectric constants are extracted as follows:

$$\begin{bmatrix} \epsilon_{\parallel m} \\ \epsilon_{\perp m} \end{bmatrix} = \begin{bmatrix} A_{\parallel e} & A_{\perp e} \\ A_{\parallel o} & A_{\perp o} \end{bmatrix}^{-1} \begin{bmatrix} f_{em}^{-2} \\ f_{om}^{-2} \end{bmatrix} \tag{10}$$

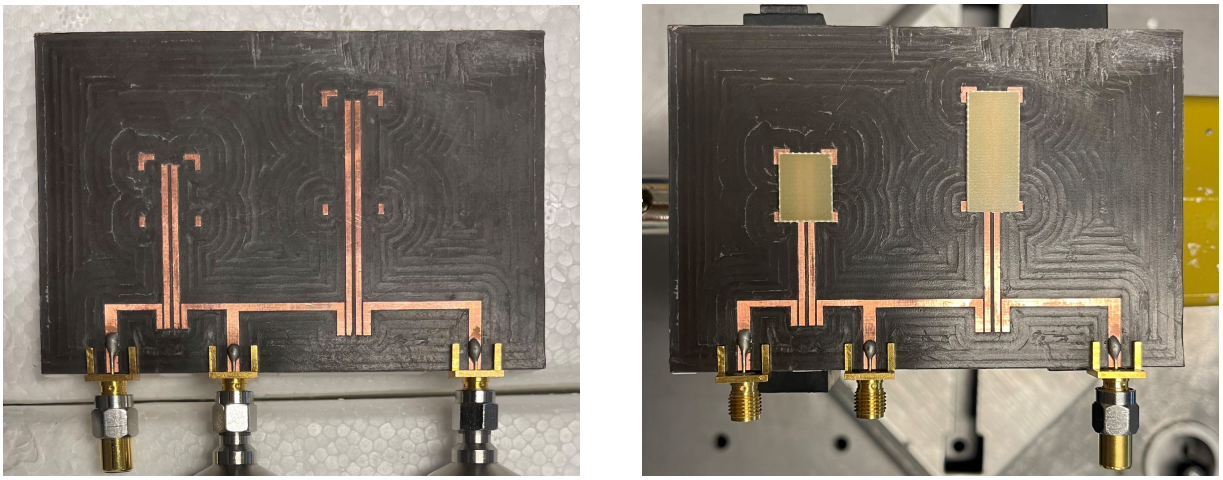

FIGURE 5. Fabricated sensor. (a) Before placing sample. (b) Loaded with Fr4 sample.

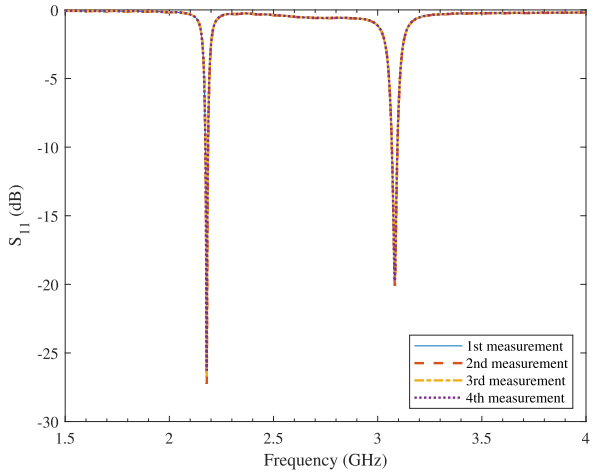

FIGURE 6. FR4 sample measured four times. The negligible difference in the measurements indicates a minimal placement error.

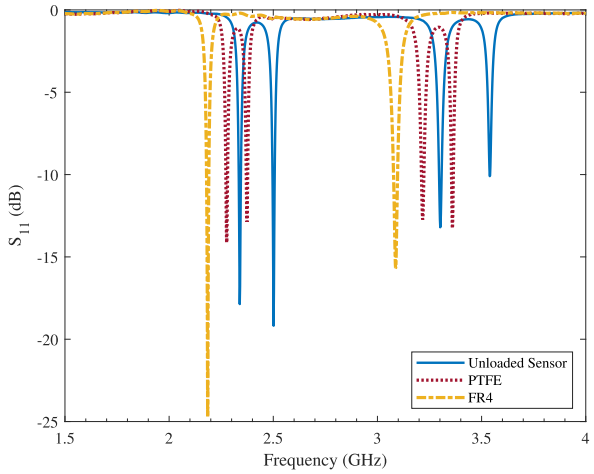

FIGURE 7. Measured S_{11} of the dual-band sensor with different samples. For FR4, the even and odd resonance frequencies are very close at both bands.

C. UNIAXIAL ANISOTROPY EXTRACTION PROCESS

To extract the permittivity tensor of anisotropic samples, the space mapping method is used. This technique relies on the mapping of the measured data to an EM full-wave simulation model. In fact, the basis of the method is adjusting the permittivity tensor components in the EM solver until the simulated result matches the measured one. The algorithm by which the space mapping is approached is introduced in the flow diagram shown in Fig. 10. This is an iterative process conducted in four stages described in detail below.

Step 1 In the first step, the fabricated sensor shown in Fig. 5 is modeled in High-Frequency Structure Simulator (HFSS). It is of significant importance to precisely model the sensor, so a good correlation between the EM simulation results and the measured data is assured.

A known source of error is a manufacturing error. To cope with this error, the fabricated sensor dimensions are measured twenty times. A caliper was used to measure the large dimensions. A scientific microscope (“AmScope MU900”) with imaging and measurement software was used to measure the small dimensions such as the gap between the coupled lines. An average of the twenty measured dimensions is considered in the EM tool.

The copper roughness is another source of error that must be taken into account in the EM model, since the copper roughness changes the effective dielectric constant [20]. Based on the provided data in the datasheet of the substrate, 2 um roughness for the dielectric side is included. The roughness of the outer copper side after fabrication is characterized using the SR160 surface roughness tester by “Starrett”, which has a 10 nm gage resolution. An average of 0.45 um copper roughness is measured, which is included in the EM model as well.

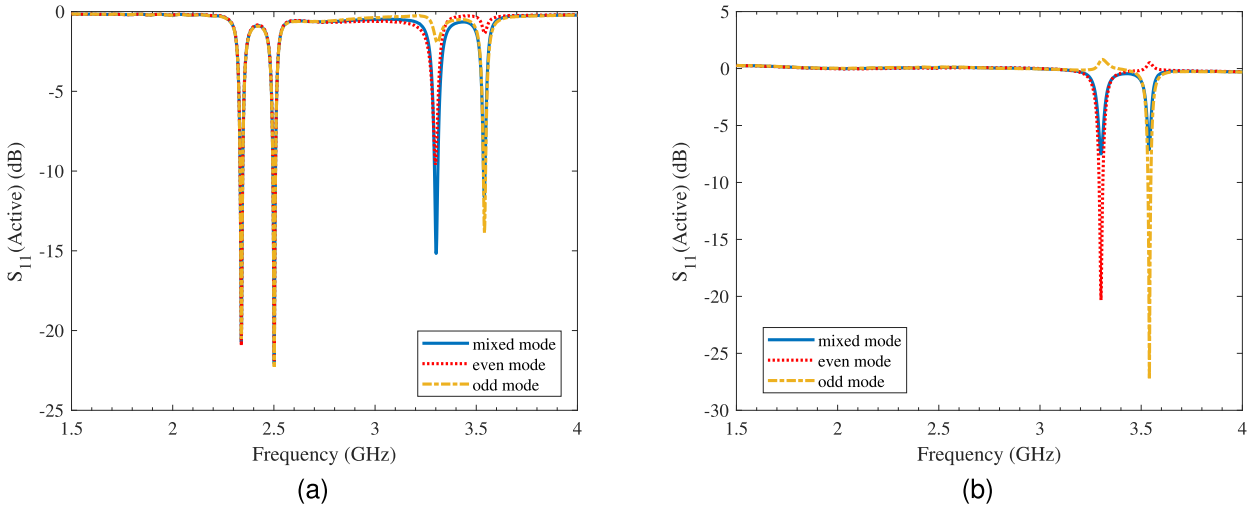

FIGURE 8. Mode separation of the first resonator. (a) Using active S_{11}. (b) Using active S_{22}.

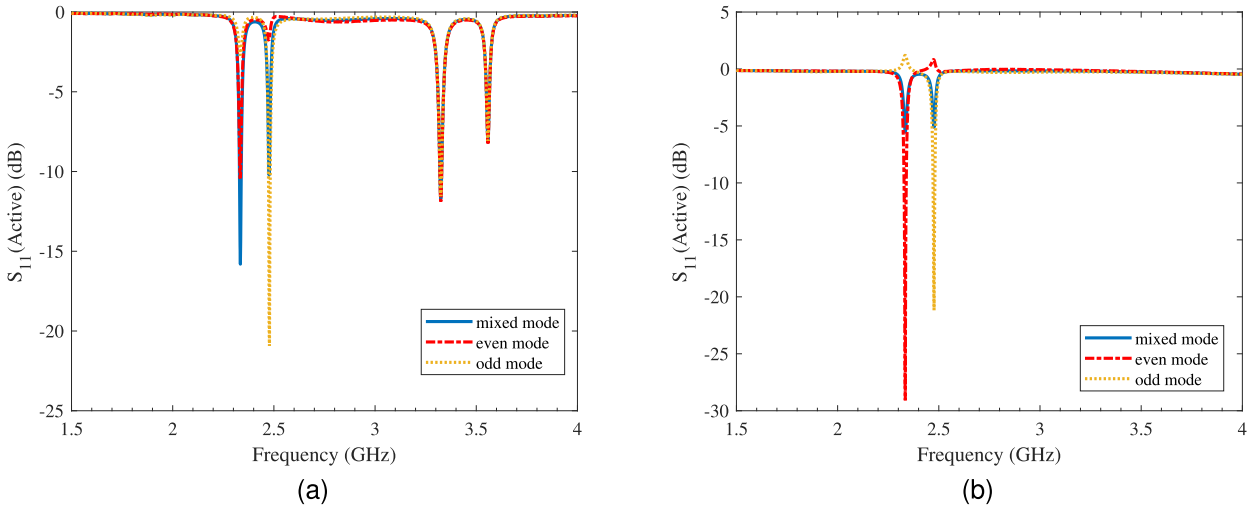

FIGURE 9. Mode separation of the second resonator. (a) Using active S_{11}. (b) Using active S_{33}.

To calibrate the sensor, the permittivity of the sensor substrate (without sample) is tuned to find the value at which the simulated resonance frequency corresponds to the measured resonance frequency. Thus, the accuracy of simulations is ensured. The permittivity of the sensor substrate (RT5880) is found at the two working frequency bands of the sensor, 2.185 at the 2.4 GHz band and 2.182 at the 3.4 GHz band. To model the different dielectric constants of the RT5880 substrate in the two frequency bands, two materials are used as the substrate in the EM model, one from port 1 to the right side of the sensor with $\epsilon_r = 2.182$ and the other one at the left side with $\epsilon_r = 2.184$.

The measured reflection coefficient at port 1 is compared to that of the simulated one in Fig. 11. The close agreement observed between them ensures the accuracy of the EM model.

Step 2 The second step is using the EM model to analyze the sensor with samples on top. Two parallel iterative processes are done to characterize the samples in two frequency bands. As shown in the flowchart, the sensor is simulated in two cases with two different permittivity tensors for the SUT. It is started with initial values assuming an isotropic SUT, $\varepsilon_{\parallel a(1)} = \varepsilon_{\perp a(1)} = \varepsilon_{ISO}$. For case b, $\varepsilon_{\parallel b(1)} > \varepsilon_{ISO}$ and $\varepsilon_{\perp b(1)} < \varepsilon_{ISO}$ is chosen. The four obtained resonance frequencies from the two simulations in cases a and b are then used in Eq. 9 to find the proportionality constant matrices.

Step 3 Next, the fabricated sensor loaded with planar samples is tested. It is worth mentioning that the surface roughness and the air gap between the SUT and sensors are the two main challenges in measuring solids with planar structures [11], [12], [13], [14], [15]. The air gap between the SUT and sensors is removed in the experiments by using

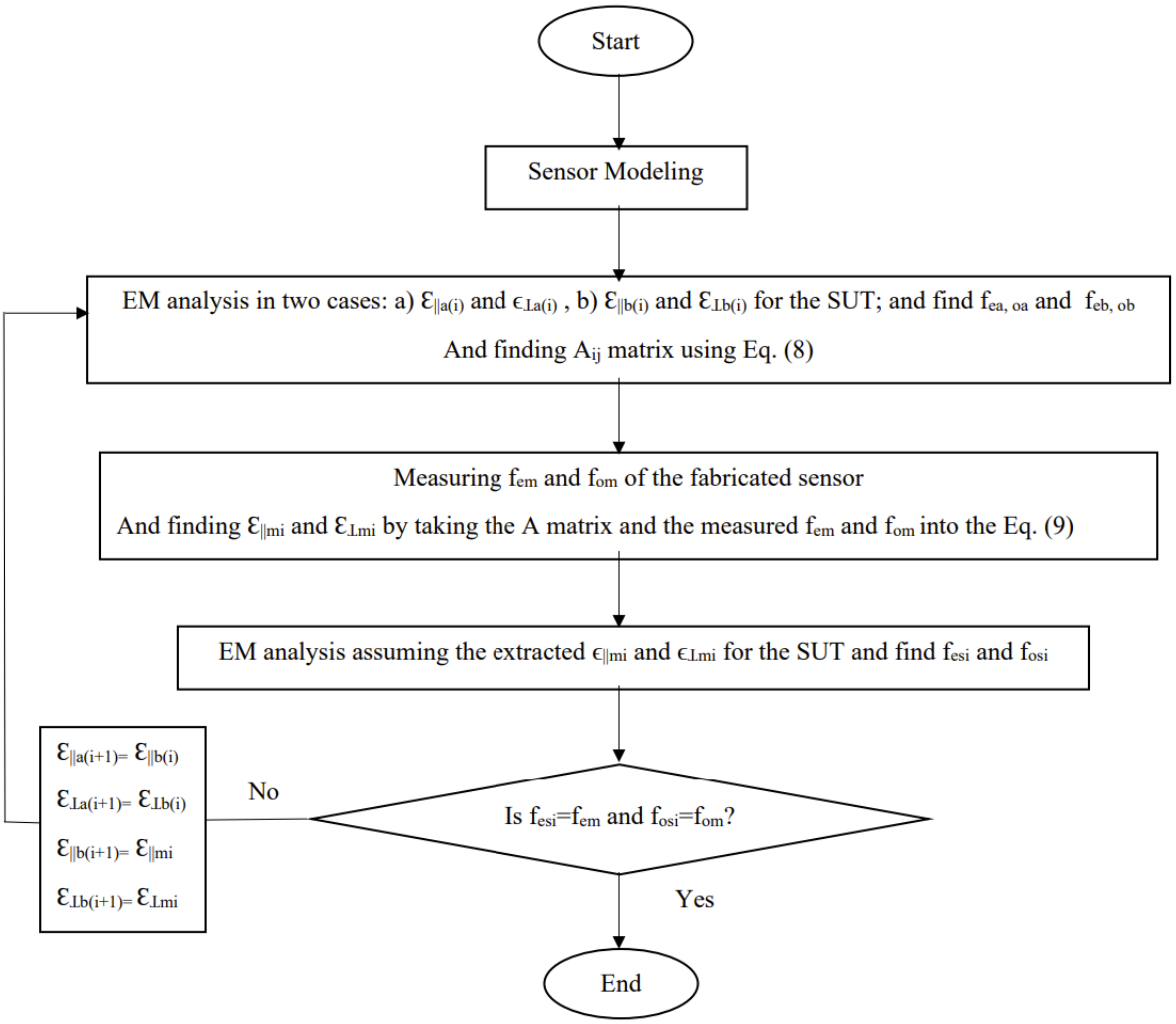

FIGURE 10. The process of uniaxial dielectric constant measurement.

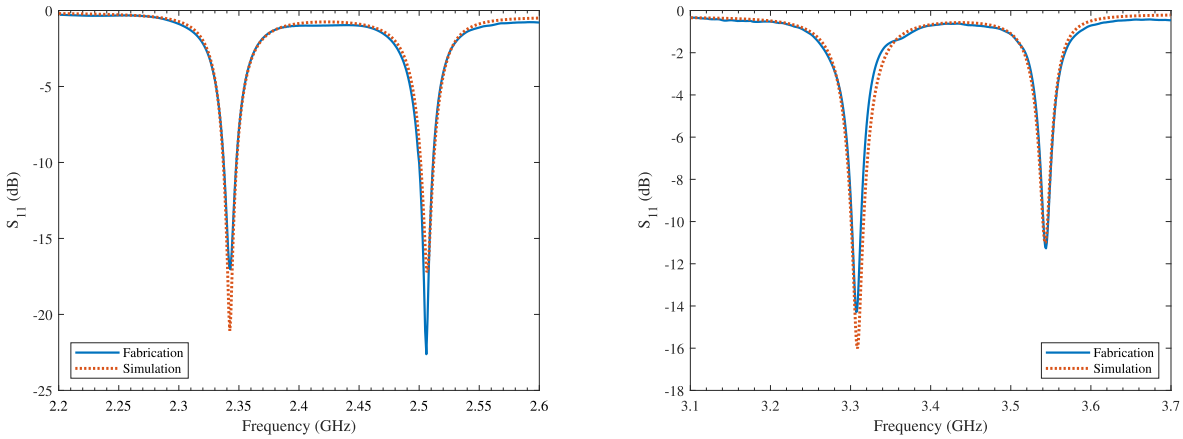

FIGURE 11. Simulated and Measured S_{11} of the sensor. (a) lower frequency band. (b) upper frequency band.

Styrofoam which is pressed over the sample and the pressure is increased until there is no change in the measured single-ended S-parameter, as was proposed in [12]. On the other hand, the surface roughness is modeled in the EM-analysis by considering an air gap layer as was proposed in [11] and [12]. The measured even and odd resonance frequencies

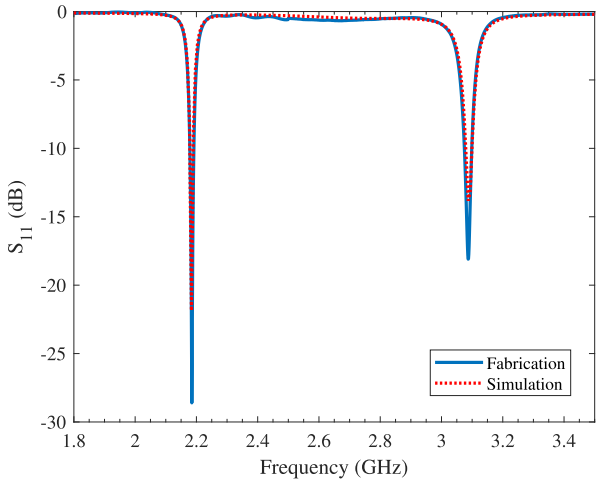

FIGURE 12. Simulated and Measured S_{11} of the sensor loaded with FR4 samples.

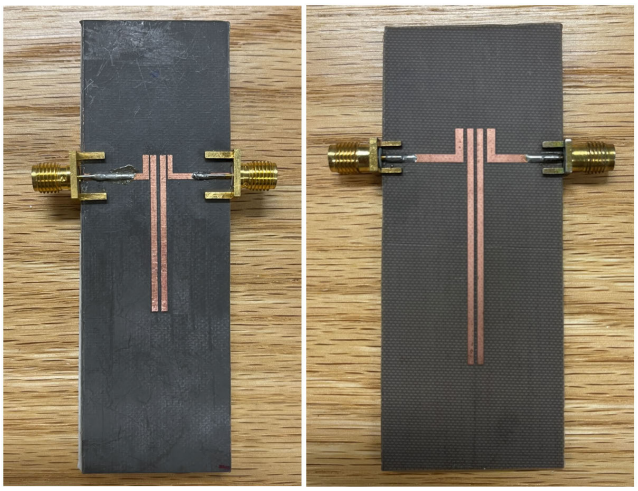

FIGURE 13. Single band sensors working at 3.4 GHz (left-hand-side) and 2.4 GHz (right-hand-side).

and the calculated A matrices are taken into Eq. 10 to find the dielectric constants $\varepsilon_{\parallel m(i)}$ and $\varepsilon_{\perp m(i)}$ at two frequency bands.

Step 4 Finally, a new EM analysis using the extracted dielectric constants is done to verify that the simulated resonance frequencies are equal to the measured ones and if they are, then the process is finished and the extracted $\varepsilon_{\parallel m(i)}$ and $\varepsilon_{\perp m(i)}$ are the actual dielectric constants of the uniaxial SUT. Otherwise, the process is repeated using the extracted $\varepsilon_{\parallel m(i)}$ and $\varepsilon_{\perp m(i)}$ as case b of the second step until convergence occurs.

For the sensor loaded with FR4 sample, the converged simulated data is compared to the measured ones in Fig. 12. The close agreement between them shows that the EM analysis is accurate enough for the loaded sensor, as well. It also demonstrates the importance of mode separation. There is only one resonance at each frequency band in the passive S-parameters, however, the even and odd resonance frequencies obtained from active S-parameters are different (f_e = 2.183 GHz and 3.081 GHz, f_o = 2.187 GHz and 3.093 GHz).

IV. EXPERIMENTAL RESULTS EVALUATION

The space mapping process is performed and two anisotropic samples of RO3010 of dimensions $L_{s1} = 13mm$ and $W_{s1} = 10mm$ for the first sample and $L_{s2} = 23mm$ and $W_{s2} = 10mm$ for the second sample are characterized in two frequency bands. By means of the surface roughness tester, the roughness of the RO3010 samples is measured 2.79 um and it is modeled as an air gap between the sample and sensor lines in the EM tool. To test the validity of the dual-band characterization, two single-band sensors, shown in Fig. 13, working at 2.4 and 3.4 GHz are also fabricated and used to measure the samples. The obtained results are compared in Table 1. The table represents the sample height, the measured even and odd mode resonance frequencies, the extracted dielectric constants, and the dielectric anisotropy ($\delta\varepsilon A$), which is defined as $\delta\varepsilon A = [2(\varepsilon_{\parallel} - \varepsilon_{\perp}) / (\varepsilon_{\parallel} + \varepsilon_{\perp})]^*100$ [21].

Using the proposed dual-band sensor, dielectric constants of the RO3010 sample are measured and the anisotropy of the sample is found 21.258 at the lower frequency band and 21.103 at the upper frequency band, yielding a difference smaller than %0.74 compared to the results obtained from the single band sensors, thus providing evidence for the accuracy of the method.

Furthermore, the dual-band sensor is used to characterize RO4003 and FR4 samples in two frequency bands. The roughness of the RO4003 and FR4 samples, 1.794 um and 0.91 um, respectively, are also modeled as an air gap in the EM analysis. The measured dielectric constants using the proposed dual-band sensor are presented and compared with prior studies in [10] and [12] in Table 2. The results of RO3010 and RO4003 characterization are fairly different from the results in [10]. This is due to the fact that first, they are measured at a different frequency and second, two different modes of a resonator are used to extract each of the parallel and perpendicular dielectric constants, so they are measured at two completely different frequencies, around 12.8 GHz for the parallel and 7.6 GHz for the perpendicular component. The anisotropy of FR4 is found to be 8.979 and 8.726 at the lower and upper frequency bands, different from the anisotropy extracted from the single band sensor in [12] by less than %3.5. The insignificant difference between the properties could be a result of the manufacturing process.

The reliability of the sensor is also tested by measuring PTFE samples with a roughness of 0.249 um and the results are compared to the ones presented in [12] in Table 2. The extracted anisotropy of PTFE, which is known to be isotropic, is found %0.142 and %0.286 at the lower and upper frequency bands, respectively. The extremely small degree of anisotropy extracted for the PTFE validates the authenticity of the method. It is worth mentioning that the proposed sensor differs from [11], [12], and [14] because the proposed circuit can measure several SUTs non-destructively at two

TABLE 1. Comparison of the extracted anisotropic permittivity components of RO3010 using double and single band sensors.

	h (mm)	f_e (GHz)	f_o (GHz)	$\varepsilon_{\parallel}$	$\varepsilon_{\perp}$	$\delta\varepsilon A$ %
Dual-band sensor (first frequency band)	1.27	2.086	1.982	11.652	9.413	21.258
single band sensor designed at 2.4 GHz	1.27	2.075	1.962	11.782	9.533	21.103
Dual-band sensor (second frequency band)	1.27	2.936	2.830	10.971	9.002	19.717
single band sensor designed at 3.4 GHz	1.27	2.903	2.790	10.965	8.995	19.739

TABLE 2. Comparison of the experimental results with previous works.

Material	h (mm)	f_em (GHz)	f_om (GHz)	$\varepsilon_{\parallel}$	$\varepsilon_{\perp}$	$\delta\varepsilon A$ %
		2.086	1.982	11.652	9.413	21.258
RO3010 (this work)	1.27	2.936	2.83	10.971	9.002	19.717
RO3010 ([10])	0.25	NA	NA	11.76	9.26	23.79
		2.18	2.252	3.670	3.369	8.552
RO4003C (this work)	1.52	3.133	3.189	3.639	3.340	8.568
RO4003C ([10])	1.52	NA	NA	3.591	3.350	6.639
RO4003C ([14])	0.79	2.347	2.495	3.67	3.37	8.52
		2.183	2.187	4.771	4.361	8.979
FR4 (this work)	1.57	3.081	3.093	4.784	4.384	8.726
FR4 ([12])	1.48	2.191	2.194	4.57	4.19	8.67
		2.277	2.375	2.110	2.107	0.142
PTFE (this work)	1.52	3.217	3.36	2.101	2.095	0.286
PTFE ([12])	1.38	2.266	2.357	2.051	2.043	0.39

independent frequency bands. Two-channel measurements reduce the error due to surrounding environmental factors such as ambient temperature [2]. The proposed sensor can also be used to simultaneously test two different samples, each at a different frequency, with a single measurement taken at the input port.

Considering isotropic samples with dielectric constants ranging from 1 to 80 in HFSS full-wave simulator, the even and odd mode resonance frequency shifts caused by isotropic dielectric constant shift are found. Based on the sensitivity definition in [22], the sensitivity of the sensor is calculated. The average sensitivity for even and odd modes is found 18.76 MHz and 27.58 MHz, respectively. Relative sensitivity is %0.8 for even mode and %1.18 for odd mode, which is comparable to the sensitivity of the recent planar sensors reviewed in [22].

V. CONCLUSION

A sensor to characterize the uniaxial anisotropic dielectric properties of solid samples at two independent frequencies is presented. The sensor is convenient to fabricate as a planar structure and consists of two dual-mode coupled-line resonators that share an input port through a T-shaped structure. The T-shaped structure isolates the two frequency bands and enables the characterization to be done by a single measurement at the input port. The different field configuration of each mode of the sensor allows for extracting parallel and perpendicular permittivity components of the SUTs placed on top of the resonators. This sensor can be used to characterize many different anisotropic samples at two distinct independent frequencies, in a non-invasive measurement setup. It can also characterize two samples, each at a different frequency, at the same time and with a single measurement at the input port. The sensor is used to determine the permittivity components of anisotropic samples of RO3010, RO4003C, and FR4. It is also used to characterize the isotropic PTFE samples to verify the validity of the results.

ACKNOWLEDGMENT

The authors would like to thank H. Banting and M. Ruphuy for useful discussions.

REFERENCES

[1] A. H. Sihvola, *Electromagnetic Mixing Formulas and Applications*, no. 47. London, U.K.: IEE, IET, 1999.

[2] R. A. Alahnomi, Z. Zakaria, Z. M. Yussof, A. A. Althuwayb, A. Alhegazi, H. Alsariera, and N. A. Rahman, "Review of recent microwave planar resonator-based sensors: Techniques of complex permittivity extraction, applications, open challenges and future research directions," *Sensors*, vol. 21, no. 7, p. 2267, Mar. 2021.

[3] L. V. Herrera-Sepulveda, J. L. Olvera-Cervantes, A. Corona-Chavez, and T. Kaur, "Sensor and methodology for determining dielectric constant using electrically coupled resonators," *IEEE Microw. Wireless Compon. Lett.*, vol. 29, pp. 626–628, 2019.

[4] M.-L. Chuang and M.-T. Wu, "Microstrip diplexer design using common T-shaped resonator," *IEEE Microw. Wireless Compon. Lett.*, vol. 21, no. 11, pp. 583–585, Nov. 2011.

[5] M. J. Akhtar, L. E. Feher, and M. Thumm, "A waveguide-based two-step approach for measuring complex permittivity tensor of uniaxial composite materials," *IEEE Trans. Microw. Theory Techn.*, vol. 54, no. 5, pp. 2011–2022, May 2006.

[6] J. Hinojosa, "Broad band electromagnetic characterization method of nematic liquid crystals using a coplanar waveguide," in *Proc. IEEE Int. Conf. Dielectric Liquids*, Jun. 2005, pp. 449–452.

[7] L. Chen, C. K. Ong, and B. T. G. Tan, "Cavity perturbation technique for the measurement of permittivity tensor of uniaxially anisotropic dielectrics," *IEEE Trans. Instrum. Meas.*, vol. 48, no. 6, pp. 1023–1030, Dec. 1999.

[8] R. G. Geyer and J. Krupka, "Microwave dielectric properties of anisotropic materials at cryogenic temperatures," *IEEE Trans. Instrum. Meas.*, vol. 44, no. 2, pp. 329–331, Apr. 1995.

[9] P. Kopyt, B. Salski, and J. Krupka, "Measurements of the complex anisotropic permittivity of laminates with TM_{0n0} cavity," *IEEE Trans. Microw. Theory Techn.*, vol. 70, no. 1, pp. 432–443, Jan. 2022.

[10] V. N. Levcheva, B. N. Hadjistamov, and P. I. Dankov, "Two-resonator method for characterization of dielectric substrate anisotropy," *Bulg. J. Phys.*, vol. 35, no. 1, pp. 33–52, 2008.
[11] J. C. Rautio and S. Arvas, "Measurement of planar substrate uniaxial anisotropy," *IEEE Trans. Microw. Theory Techn.*, vol. 57, no. 10, pp. 2456–2463, Oct. 2009.
[12] H.-N. Morales-Lovera, J.-L. Olvera-Cervantes, A. Corona-Chavez, and T. K. Kataria, "Dielectric anisotropy sensor using coupled resonators," *IEEE Trans. Microw. Theory Techn.*, vol. 68, no. 4, pp. 1610–1616, Apr. 2020.
[13] B. J. Rautio, M. E. Sabbagh, and J. C. Rautio, "Detailed error analysis and automation of the RA resonator technique for measurement of uniaxial anisotropic permittivity," in *Proc. 78th ARFTG Microw. Meas. Conf.*, Dec. 2011, pp. 1–5.
[14] H.-N. Morales-Lovera, J.-L. Olvera-Cervantes, A.-E. Perez-Ramos, A. Corona-Chavez, and C. E. Saavedra, "Microstrip sensor and methodology for the determination of complex anisotropic permittivity using perturbation techniques," *Sci. Rep.*, vol. 12, no. 1, pp. 1–8, Feb. 2022.
[15] J. C. Rautio, "Measurement of uniaxial anisotropy in Rogers RO3010 substrate material," in *Proc. IEEE Int. Conf. Microw., Commun., Antennas Electron. Syst.*, Nov. 2009, pp. 1–4.
[16] S. Kiani, P. Rezaei, and M. Navaei, "Dual-sensing and dual-frequency microwave SRR sensor for liquid samples permittivity detection," *Measurement*, vol. 160, Aug. 2020, Art. no. 107805.
[17] M. Kirschning and R. H. Jansen, "Accurate wide-range design equations for the frequency-dependent characteristic of parallel coupled microstrip lines," *IEEE Trans. Microw. Theory Techn.*, vol. MTT-32, no. 1, pp. 83–90, Jan. 1984.
[18] H. Lee, J. Yousaf, J. Kim, W. Nah, J. Youn, D. Lee, and C. Hwang, "Analysis of antenna performance degradation due to VCO source using active S-parameters," in *Proc. Int. Symp. Electromagn. Compat. (EMC EUROPE)*, Aug. 2018, pp. 951–956.
[19] C. Zhang, Q. Lai, and C. Gao, "Measurement of active S-parameters on array antenna using directional couplers," in *Proc. IEEE Asia Pacific Microw. Conf. (APMC)*, Nov. 2017, pp. 1167–1170.
[20] A. F. Horn, J. W. Reynolds, and J. C. Rautio, "Conductor profile effects on the propagation constant of microstrip transmission lines," in *IEEE MTT-S Int. Microw. Symp. Dig.*, May 2010, pp. 868–871.
[21] P. I. Dankov, "Dielectric anisotropy of modern microwave substrates," in *Microwave and Millimeter Wave Technologies From Photonic Bandgap Devices to Antenna and Applications*. Bulgaria: IntechOpen, 2010.
[22] M. Abdolrazzaghi, V. Nayyeri, and F. Martin, "Techniques to improve the performance of planar microwave sensors: A review and recent developments," *Sensors*, vol. 22, no. 18, p. 6946, Sep. 2022.

SHABNAM AHMADI ANDEVARI received the B.Sc. degree in electrical engineering from the Babol Noshirvani University of Technology, Babol, Iran, in 2014, and the M.Sc. degree in electrical engineering, fields and waves from the Amirkabir University of Technology, Tehran, Iran, in 2017. She is currently pursuing the Ph.D. degree with Queen's University, Kingston, ON, Canada. Her research interests include material characterization and inclination sensors using microwave technology.

JOSE-LUIS OLVERA-CERVANTES received the B.Sc. degree from the Instituto Politécnico Nacional, Mexico City, Mexico, in 2001, and the M.Sc. and Ph.D. degrees from the Centro de Investigación Científica y de Educación Superior de Ensenada, Ensenada, Mexico, in 2005 and 2008, respectively. In 2009, he joined with the Instituto Nacional de Astrofísica, Óptica y Electrónica, where he is currently a Full Professor. His research interests include microwave sensors, radar systems, dielectric characterization, food properties, and signal processing.

HECTOR-NOEL MORALES-LOVERA was born in Tabasco, Mexico. He received the B.Ing. degree in mechatronics from the Instituto Tecnologico Superior de Comalcalco (ITSC), in 2017, and the master's degree in electronics from the National Institute of Astrophysics, Optics and Electronics (INAOE), where he is currently pursuing the Ph.D. degree in electronics, characterizing materials using microwaves, RF circuits design, and metamaterials.

CARLOS E. SAAVEDRA received the Ph.D. degree in electrical engineering from Cornell University, Ithaca, New York. He is a Professor and the Head of the Department of Electrical and Computer Engineering with Queen's University, Kingston, ON, Canada. He is a licensed Professional Engineer (P.Eng.) in Ontario. He is a former Co-Chair of the NSERC Discovery Grants Evaluation Group 1510 and he has served on grant review panels at the U.S. National Science Foundation. He is a former Associate Editor of the IEEE TRANSACTIONS ON MICROWAVE THEORY AND TECHNIQUES, Guest Editor of the IEEE OPEN JOURNAL OF ANTENNAS AND PROPAGATION and Guest Editor of the IEEE *Microwave Magazine*.